

Article

A HepG2 Cell-Based Biosensor That Uses Stainless Steel Electrodes for Hepatotoxin Detection

Martin Rozman ^{1,2,†}, Zala Štukovnik ^{1,†}, Ajda Sušnik ^{1,3}, Amirhossein Pakseresht ², Matej Hočevar ^{4,5}, Damjana Drobne ⁴ and Urban Bren ^{1,6,*}

¹ Faculty of Chemistry and Chemical Engineering, University of Maribor, 2000 Maribor, Slovenia; martin.rozman@tnuni.sk (M.R.); zala.stukovnik1@um.si (Z.Š.); ajda.susnik@nib.si (A.S.)

² FunGlass—Center for Functional and Surface Functionalized Glass, Alexander Dubček University of Trenčín, 91150 Trenčín, Slovakia; amir.pakseresht@tnuni.sk

³ National Institute of Biology, 1000 Ljubljana, Slovenia

⁴ Biotechnical Faculty, University of Ljubljana, 1000 Ljubljana, Slovenia; matej.hocivar@imt.si (M.H.); damjana.drobne@bf.uni-lj.si (D.D.)

⁵ Institute of Metals and Technology, 1000 Ljubljana, Slovenia

⁶ Natural Sciences and Information Technologies, Faculty of Mathematics, University of Primorska, 6000 Koper, Slovenia

* Correspondence: urban.bren@um.si

† These authors contributed equally to this work.

Abstract: Humans are frequently exposed to environmental hepatotoxins, which can lead to liver failure. Biosensors may be the best candidate for the detection of hepatotoxins because of their high sensitivity and specificity, convenience, time-saving, low cost, and extremely low detection limit. To investigate suitability of HepG2 cells for biosensor use, different methods of adhesion on stainless steel surfaces were investigated, with three groups of experiments performed in vitro. Cytotoxicity assays, which include the resazurin assay, the neutral red assay (NR), and the Coomassie Brilliant Blue (CBB) assay, were used to determine the viability of HepG2 cells exposed to various concentrations of aflatoxin B1 (AFB1) and isoniazid (INH) in parallel. The viability of the HepG2 cells on the stainless steel surface was quantitatively and qualitatively examined with different microscopy techniques. A simple cell-based electrochemical biosensor was developed by evaluating the viability of the HepG2 cells on the stainless steel surface when exposed to various concentrations of AFB1 and INH by using electrochemical impedance spectroscopy (EIS). The results showed that HepG2 cells can adhere to the metal surface and could be used as part of the biosensor to determine simple hepatotoxic samples.

Keywords: HepG2 cell line; impedance biosensor; adhesion; hepatotoxins; stainless steel



Citation: Rozman, M.; Štukovnik, Z.; Sušnik, A.; Pakseresht, A.; Hočevar, M.; Drobne, D.; Bren, U. A HepG2 Cell-Based Biosensor That Uses Stainless Steel Electrodes for Hepatotoxin Detection. *Biosensors* **2022**, *12*, 160. <https://doi.org/10.3390/bios12030160>

Received: 11 February 2022

Accepted: 2 March 2022

Published: 4 March 2022

Publisher's Note: MDPI stays neutral with regard to jurisdictional claims in published maps and institutional affiliations.



Copyright: © 2022 by the authors. Licensee MDPI, Basel, Switzerland. This article is an open access article distributed under the terms and conditions of the Creative Commons Attribution (CC BY) license (<https://creativecommons.org/licenses/by/4.0/>).

1. Introduction

Acute and chronic liver diseases are significant global health problems. In addition to liver damage caused by unhealthy lifestyles and viruses including hepatitis A, B, C, D, and E viruses, humans are frequently exposed to environmental hepatotoxins that can cause liver failure, acute cellular damage, or chronic diseases such as fibrosis and liver cancer [1]. Hepatotoxins include mycotoxins such as aflatoxins, which are the key concern in the food industry [2,3] and are mainly produced by *Aspergillus flavus* and *Aspergillus parasiticus* [4]. Examples of hepatotoxins include monomethylhydrazine, amatoxins, orellanine [5] and amanitin, commonly present in the fungal families of *Agaricaceae* (genus *Lepiota*) or *Amanitaceae* (genus *Amanita*). One of the most deadly mushrooms is *Amanita phalloides*, commonly referred to as the death cap, which has the highest concentration of amatoxins α -, β -, and γ -amanitin compared to other fungal families [6]. To date, no specific antidote exists for amanitin poisoning, and treatment is limited to support (dialysis, activated charcoal hemoperfusion, glucose/saline perfusion, etc.), or in the worst case,

requires a liver transplant [5]. Another case of hepatotoxin represents a large variety of therapeutic drugs such as paracetamol [7], which is commonly used as pain relief medication and numerous antibiotics such as isoniazid (INH), which is often used for the treatment of more aggressive bacterial infections such as tuberculosis [8]. While INH is not directly hepatotoxic, its metabolites (e.g., acetyl hydrazine and hydrazine), along with interference with different enzymes (e.g., cytochrome P450), enables it to become harmful [9,10].

To detect harmful compounds or other analytical species, there are several methods for the detection of hepatotoxins including enzyme-linked immunosorbent assay (ELISA), high-performance liquid chromatography (HPLC), and liquid chromatography-mass spectrometry (LC-MS/MS) [11]. However, these methods require expensive equipment and are labor-intensive with regard to sample preparation [12].

One alternative is biosensors, which are small and inexpensive analytical devices that convert a biological response into an electrical signal and provide us with information about the concentration of the target analyte [13,14].

The quality of this information depends on the type of analyte components, the type of active biological component, the design of the biosensor, and the physical properties of the transducer [15]. Based on the transducer, biosensors can be classified into electrochemical, optical, and mechanical, which use an active biological component [16]. Active biological components can generally be enzymes, antibodies, *in vitro* cells, organelles, or tissues [17].

Many biosensors have been developed over the years that utilize cells for environmental monitoring, detection of pathological biomarkers, and cell culture monitoring [18–24]. Living cells have been used as biorecognition elements in biosensors since the early 1970s. They are an interesting choice of bioreceptor because they are cheaper than purified enzymes and antibodies, allow for flexibility in determining the sensing strategy, and are relatively easy and inexpensive to manufacture. However, cells can have a relatively short storage life and can be difficult to adhere to the surface [25]. Human hepatocellular carcinoma cell line (HepG2), a line derived from a human hepatoblastoma, has been found to express a variety of liver-specific metabolic functions, and is therefore a suitable candidate for biosensing applications that could mimic the liver tissue environment [26]. These cells perform many metabolic functions such as the use of the cytochrome P450 family of enzymes [27], which serve by selectively catalyzing the oxidation or reduction of chemical species as well as converting less water-soluble chemical species into smaller and more soluble metabolites [28]. As such, HepG2 cells present an excellent candidate for biosensor application, where initial chemicals are relatively harmless, but are transformed into more toxic components after their transformation.

Besides the biorecognition element, a fundamental part of a biosensor is the signal transduction mechanism through which binding events are converted into detectable and quantifiable physical signals [29]. Label-free biosensors measure integrated and phenotypic responses of whole cells with high temporal resolution. Furthermore, these biosensors enable noninvasive and highly sensitive measurements of many different cellular responses, ranging from cell adhesion, migration, differentiation, and even different types of cell death [30,31]. Optical and electrochemical biosensors are considered as label-free methods and enable real-time monitoring of the binding reaction, hence giving access to the kinetic parameters of the molecular recognition process [32,33]. In general, the factors that help in determining a particular immobilization strategy for a biosensor include the cell types used as bioreceptors, the type of material or substrate onto which cells are to be immobilized, the toxicity of the substrate, cell viability, growth requirements, and the application of the biosensor [25,34]. As a substrate surface, the most commonly used materials for biosensor development include inert metals, metal oxides, carbon-based materials (glassy carbon, graphite), and organic electroconductive polymers [35]. An interesting material represents stainless steel, since it has excellent chemical and electrical properties as well as physical and mechanical characteristics. These characteristics depend on how the steel is prepared, where it can be in different shapes such as bars, plates, or even foil. In addition to different forms, there are numerous types of steel alloys that can be used regarding the specific

requirements. In the form of metal foil, this material is extremely easy to work with and has been used in a variety of electrochemical and optoelectronic devices. From an economical point, steel foil is cheaper in terms of the material cost and required tooling for its processing.

Electrochemical impedance spectroscopy (EIS) is widely used in electrochemical sensors and biosensors as a diagnostic and quantitative nondestructive detection method [36]. The measurement comprises the real (electric resistance) and imaginary (capacitance) components of the impedance response of an electrochemical system [37,38]. With electrochemical impedance spectroscopy, the frequency response of the electric current is measured, and thus the data on the living cells and the coverage of the electrode surface is obtained [39]. Under the electric fields, the cellular plasma membrane acts as an insulating barrier, directing the current to flow between or beneath the cells, leading to extracellular and transcellular currents. The extracellular current is primarily due to the intercellular conduction, while the transcellular current results from the control of cell-membrane capacitance [31]. The electrochemical impedance spectroscopy allows us to characterize the cells immobilized to the electrodes and the analyte present in the sample and due to its rapid response, it can be used to monitor molecular events in real-time [40]. Nevertheless, when designing a novel type of biosensor, different morphological or spectroscopical methods, along with cytotoxicity tests, have to be used in order to validate EIS measurements and to ensure that the device indeed has a desired response. There have been reports of biosensors that used HepG2 cells adhered to the surface [41], however, these were adhered to screen-printed carbon electrodes (SPCE), which is more difficult to prepare or modify, compared to metal electrodes.

In this paper, the authors present the use of HepG2 cells adhered to a stainless steel surface to be used as a working electrode in an electrochemical biosensor that uses the EIS method to detect different hepatotoxins such as isoniazid (INH) and aflatoxin B1 (AFB1). Cytotoxicity of both hepatotoxins was investigated, along with morphological properties of the cell-covered steel electrode and its use in the electrochemical system by the means of electrochemical impedance spectroscopy. The biosensor only uses stainless steel electrodes, greatly reducing the cost of manufacture. The data presented here, on two different chemical substances, could serve as a baseline for further improvements in order to make a biosensor that will be able to detect different varieties of hepatotoxins.

2. Materials and Methods

All chemicals were purchased from Sigma-Aldrich and SPI supplies, and in all cases had a purity of 98% or higher. The cells were applied to AISI 316 stainless steel (TBJ GmbH, Germany) foil. The water was purified using a Seralpur Pro 90C unit in combination with a USF Elga laboratory unit. Insulating tape (Tesa, Germany) and adsorption paper (MultiFun Paloma, Slovenia) were purchased locally. Aflatoxin B1 (AFB1) primary solution was prepared by dissolving 1 mmol of AFB1 along with 50 μ L of DMSO and 4 mL of deionized water. Isoniazid (INH) primary solution was prepared by dissolving 1 mol of INH in 4 mL of deionized water. Both primary solutions were diluted with deionized water as required.

2.1. Cytotoxic Tests

To determine cell viability, the neutral red (NR) dye uptake test, and the Coomassie Brilliant Blue (CBB) dye test were performed *in vitro* on the HepG2 cell line.

The neutral red uptake assay provides a quantitative estimation of the number of viable cells in cell culture and the staining procedure was carried out according to the literature [42].

The Coomassie Brilliant Blue dye test was used as a protein determination method and performed according to the staining procedure obtained from the literature [43].

For staining, two 96-well plates with cells seeded at a density of approximately 8000 cells/spot (40,000 cells/mL) were prepared and incubated overnight at 37 °C and a 5% CO₂ atmosphere. The cells adhered to the surface of the plate. After 24 h, aflatoxin B1

(AFB1) at concentrations of 0.1, 1, 10, 20, 50, 100, 250 μM , isoniazid (INH) at concentrations of 5, 10, 50, 100, 150, 200, 250 mM, and the negative control were prepared. The cells were exposed to the different concentrations of AFB1 and INH for 24 h. After exposure to toxins, the dyes were applied to selected individual wells and were left for a selected amount of time according to individual staining procedure before being used for further investigation. The dyed plates were investigated using a UV-Vis spectrofluorometer (BioTek, Cytation 3).

Furthermore, the resazurin test was also performed to confirm that both the neutral red and Coomassie Brilliant Blue method showed the correct results.

The reaction manifests through a visual color change from blue to a spectrum ranging from dark purple to pink [44]. The results for the resazurin dye are presented in the Supplementary Materials along with the measurement in the figure of Section 3.5 (Figure S1).

2.2. Optical Microscopy

Qualitative analysis of cell viability was carried out using an optical microscope Axio (Zeiss, Germany). Cells were seeded with a density of 1.5×10^4 cells/cm² (2.78×10^4 cells/mL) in two different 12-well plates and were incubated for 48 h at 37 °C and a 5% CO₂ atmosphere. Cells were exposed to AFB1 at concentrations of 5, 50, and 250 μM and to INH at concentrations of 5, 50, and 150 mM for 24 h. Afterward, a qualitative exposure analysis of cell viability was carried out. All optical microscopy measurements were performed at 20 \times times magnification.

2.3. Fluorescence Microscopy

Analysis of cell viability was further carried out using a fluorescent microscope AxioImager Z1 (Zeiss, Germany). Fluorescence microscopy is a technique by which fluorescent substances are examined through a microscope. This has several advantages over other forms of microscopy, offering high sensitivity and specificity. In fluorescence microscopy, the specimen is illuminated with light of a relatively short wavelength, usually ultraviolet [45].

The 0.050 mm thick stainless steel plates with a 5 mm \times 15 mm surface were first disinfected under UV light. Cells were seeded at a density of 1.5×10^4 cells/cm² (2.78×10^4 cells/mL) on stainless steel plates and incubated for 48 h at 37 °C and a 5% CO₂ atmosphere. Cells were exposed to AFB1 at concentrations of 5, 50, and 250 μM and to INH at concentrations of 5, 50, and 150 mM. After 24 h, the cell plates were washed with Dulbecco's saline phosphate solution (PBS), which removed the detached cells. The cells were dyed with 2 $\mu\text{g}/\text{mL}$ Hoechst 33242 and 2 $\mu\text{g}/\text{mL}$ propidium iodide. Hoechst 33242 stains the nuclei of all cells blue, and propidium iodide stains the nuclei of cells with damaged plasma red. Quantitative analysis was performed using image assessment software (ImageJ 1.53k) based on the number of viable cells (blue colored) and the number of non-viable cells (red colored) on the steel surface. All fluorescence microscopy measurements were performed at 40 \times times magnification.

2.4. Scanning Electron Microscopy

After observing the adhesion of the cells on the stainless steel surface and cell viability with an optical microscope and fluorescence microscope, the surfaces with adhered cells were further prepared for scanning electron microscopy (SEM).

Surfaces with adhered cells were washed in phosphate buffer (PBS) for 30 min. Afterward, the cells on the surfaces were immersed for 48 h at 4 °C in Karnovsky fixative, prepared from 2.5% glutaraldehyde (SPI Supplies, West Chester, PA, ZDA), and 0.4% paraformaldehyde (Merck KGaA, Darmstadt, Germany) in 1 M NaH₂PO₄·2H₂O and Na₂HPO₄·2H₂O (Merck KGaA, Darmstadt, Germany). Cells were washed with 1 M phosphate buffer saline, fixed with 1% OsO₄ (SPI Supplies, West Chester, PA, USA), and rinsed with distilled water. The cell surfaces were washed in an oversaturated and filtered tiorbohydrazide (TCH) solution, rinsed with distilled water, fixed with 1% OsO₄, and rinsed

again with distilled water. Samples were dehydrated with ethanol at concentrations of 30%, 50%, 70%, 80%, 90%, and absolute ethanol (Merck KGaA, Darmstadt, Germany). Further dehydration rates were performed with a mixture of hexamethyldisiloxane (HMDS; SPI Supplies, West Chester, PA, USA) and absolute ethanol in a ratio of 1:2 and ratio of 1:1, and with the absolute HMDS. After 24 h, samples were resurfaced with a 6 nm thick coat of Au/Pd using a precision etching and coating system (PECS). Scanning electron microscopy was carried out to visualize the morphology of adhered HepG2 cells on stainless steel surfaces using a scanning electron microscope JSM-7600 F (JEOL, Tokyo, Japan). Microphotographs were recorded at 100 \times , 1000 \times , and 5000 \times magnification.

2.5. Biosensor Assembly and Electrochemical Impedance Spectroscopy (EIS)

Stainless steel plates with a surface area 5 mm \times 15 mm and thickness of 0.050 mm were disinfected under UV light. Cells were seeded at a density of 3×10^4 cells/cm² (5.55×10^4 cells/mL) on stainless steel plates and incubated for 48 h at 37 °C and 5% CO₂ atmosphere. After 48 h, the cells were exposed to AFB1 at a concentration of 250 μ M and to INH at a concentration of 150 mM. After 24 h, the plates covered with cells were washed with Dulbecco's saline phosphate solution (PBS), which removed the detached cells. A three-electrode system with stainless steel electrodes was assembled. The device was constructed similarly to most commercial three-electrode electrochemical biosensors, utilizing flat electrodes placed in a planar configuration. The three-electrode system included the working electrode (WE) with HepG2 cells as a biological component, reference electrode (RE), and counter electrode (CE). For all three electrodes, stainless steel foil type 316 was used, with the WE being modified with HepG2 cells, while RE and CE were unmodified stainless steel foils. Electrodes were placed on a flat surface with a piece of insulation tape attached to the entire bottom of each electrode. After insulator attachment, they were positioned horizontally to each other with a 1 mm gap, in order to prevent a short circuit. A piece of adsorption paper with dimensions of 5 mm \times 17 mm was placed on top of the electrodes in such way that each electrode had an active area of 5 mm \times 5 mm. A phosphate buffer solution (PBS) was used as the electrolyte and was carefully dripped onto adsorption paper until it was soaked.

For the evaluation of electrochemical cells, the electrochemical impedance spectroscopy method (EIS) was used [46]. The measurements were carried out with a PalmSens4 potentiostat/galvanostat with a frequency range from 50 kHz to 0.1 Hz with 9.5 points per decade, totaling 55 points per measurement. The stability of the three-electrode system with HepG2 cells was previously determined by measuring the potential of the open circuit (OCP), where the potential difference between the reference electrode (RE) and the working electrode (WE) was measured.

3. Results

3.1. Cytotoxic Tests

The neutral red assay showed that AFB1 causes statistically significant changes in the lysosomal integrity of HepG2 cells at concentrations above 10 μ M and that the INH causes changes in lysosomal integrity at concentrations above 10 mM and the changes can be observed in Figure 1A,B, where the decrease in the cell viability with increasing hepatotoxin concentration is shown. The Coomassie Brilliant Blue assay showed similar results (Figure 1C,D) compared to the neutral red assay, indicating that both methods imply that both compounds indeed have a hepatotoxic response. Similarly to data presented in the neutral red test, AFB1 concentrations above 10 μ M showed a reduction in the number of cells in the cell population and that INH concentrations above 10 mM also had a significant effect on the number of cells.

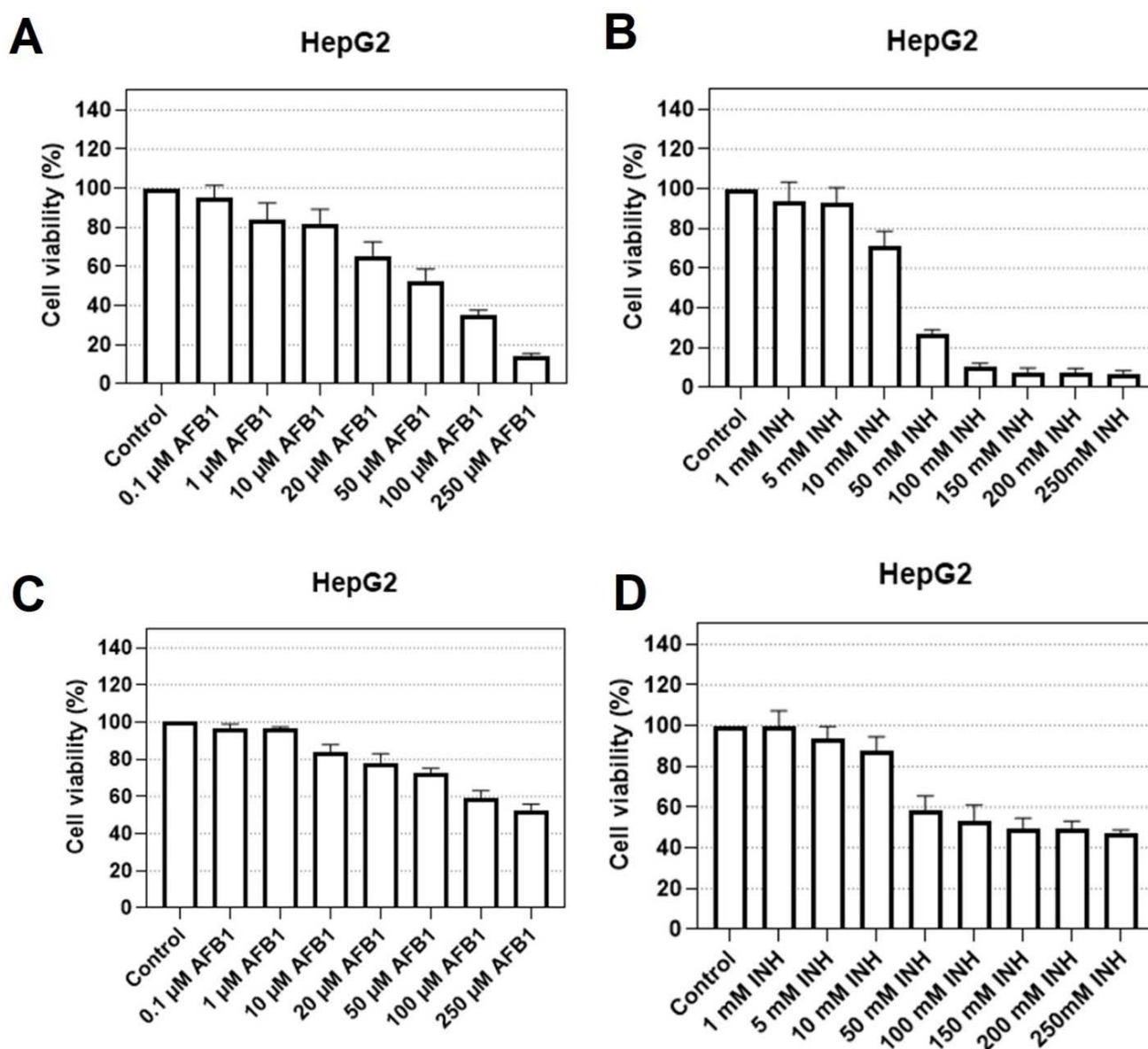


Figure 1. The HepG2 cell viability after exposure to various concentrations of AFB1 (A) and INH (B) when stained with neutral red and cell viability following the Coomassie Brilliant Blue staining test for AFB1 (C) and INH (D). The results are given as mean values of the three measurements \pm STD ($p < 0.001$).

Overall, the cytotoxic assays showed that AFB1 had significant effects on cell proliferation and viability at concentrations exceeding 10 μ M, while INH showed effects at concentrations above 10 mM. The results were used to determine what concentration range is expected for an individual substance to have an effect and to assess the limit of detection (LOD) for the investigated biosensor.

3.2. Optical Microscopy

The surface of the glass plate had good coverage with the HepG2 cell population. In comparison, HepG2 cells had progressively lower cell coverage on the plate after exposure to increasing concentrations of AFB1 and increasing concentrations of INH. Although all hepatocytes appeared to be homogeneous under the light microscope, it can be seen that the cells in the different zones showed structural and functional heterogeneity. The photomicrographies for both hepatotoxins are presented in Figure 2. For AFB1 exposure (Figure 2A–D), it can be observed that the gaps between the cells increased, which indicates

that their affinity toward tissue structure tendency was reduced. At a concentration of 50 μM , AFB1 cells began to individualize, suggesting that they were less able to proliferate, with an increasing number of smaller, cell-like structures, suggesting that some of the cells had started the cell death process [47]. At the highest concentration (250 μM AFB1), the only visible structures were blebs and cell residues that appear during the cell death process. Similar damage could be observed in the case of INH (Figure 2E–H), where at the initial concentration (5 mM INH), cell proliferation was again decreased, and at higher concentrations (50 mM and 250 mM), smaller structures could be observed, which could be due to cell necrosis caused by the increased INH concentration.

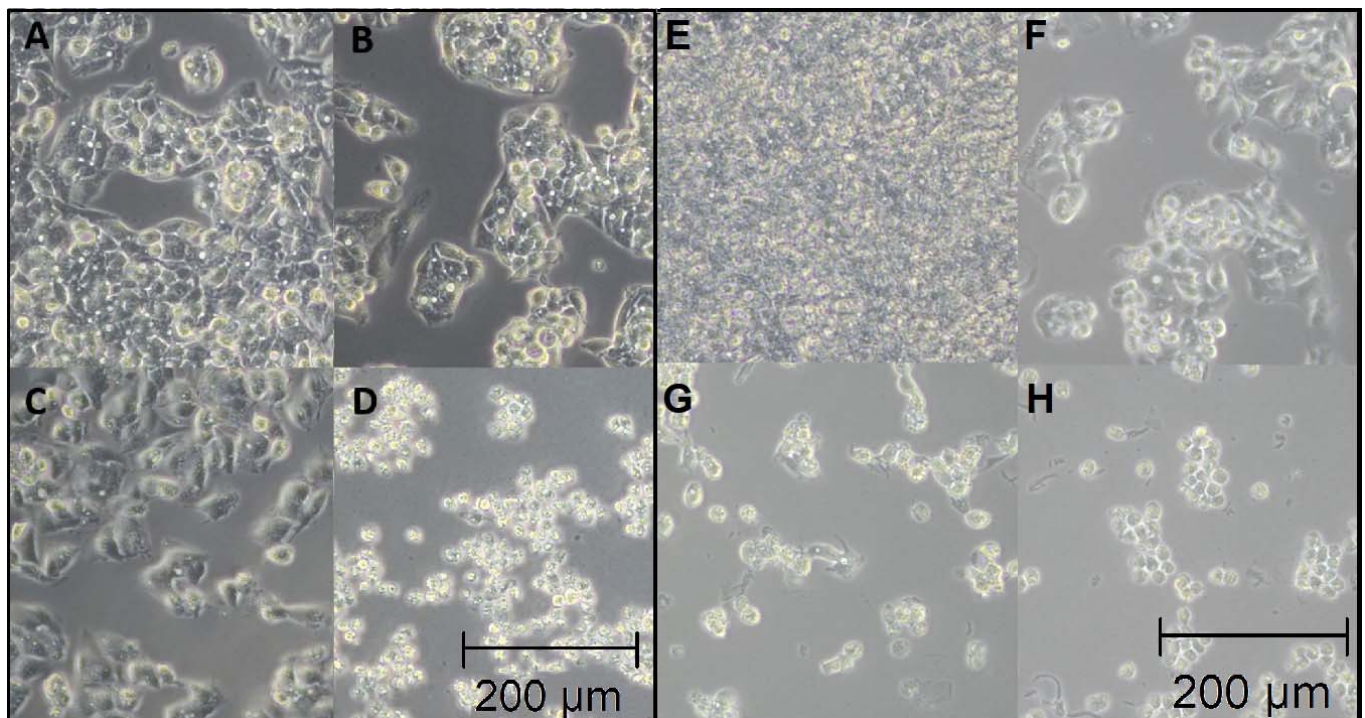


Figure 2. Optical microscopy photographs under the influence of AFB1 on the HepG2 cell line (A–D) exposed to different concentrations for the control (A), 5 μM (B), 50 μM (C), and 250 μM (D) AFB1 concentrations. A similar investigation was conducted for INH (E–G) showing the control (E), 5 mM (F), 50 mM (G), and 250 mM (H) INH concentration. For all photographs, magnification was 20 \times .

3.3. Fluorescence Microscopy

Using fluorescence microscopy, cell survival was quantitatively determined by counting all cells in the cell population (blue cell nucleus) and dead cells (red cell nucleus). Two different staining agents were used for this purpose: Hoechst 33342 stains the nucleus of all cells blue, and propidium iodide stains the nucleus of cells with damaged plasma red. The difference between the number of all cells and the dead cells in the cell population was calculated to obtain the number of all living cells in the cell population (the difference between blue and red nuclei). Fluorescence photomicrographs are presented in the Supplementary Materials Figures S2 and S3. For both AFB1 and INH, the results showed that the HepG2 control had a high concentration of adherent cells on the steel surface throughout the cell population. The number of live cells on the steel surface was relatively high compared to the total cell population, while the number of dead cells on the stainless steel surface was quite low when observing cells in the control group. The number of all cells in the whole cell population and the number of live HepG2 cells on the steel surface after exposure to increasing AFB1 concentrations of 5, 50, and 250 μM decreased, consequently, the number of dead cells at increasing concentrations of AFB1 gradually

increased compared to the control. In comparison, HepG2 cells showed progressively lower cellular steel coverage after exposure to increasing concentrations of AFB1, which was expected due to its hepatotoxicity. For INH investigation, the number of dead cells gradually increased at concentrations of 5 and 50 mM compared to the control. At an INH concentration of 250 mM, dead cells on the stainless steel surface appeared to be lower than at an INH concentration of 50 mM, which could be due to detachment of the cells or their complete necrosis due to the high concentration of INH. Graph of counted cells during fluorescence microscopy is presented in Figure 3.

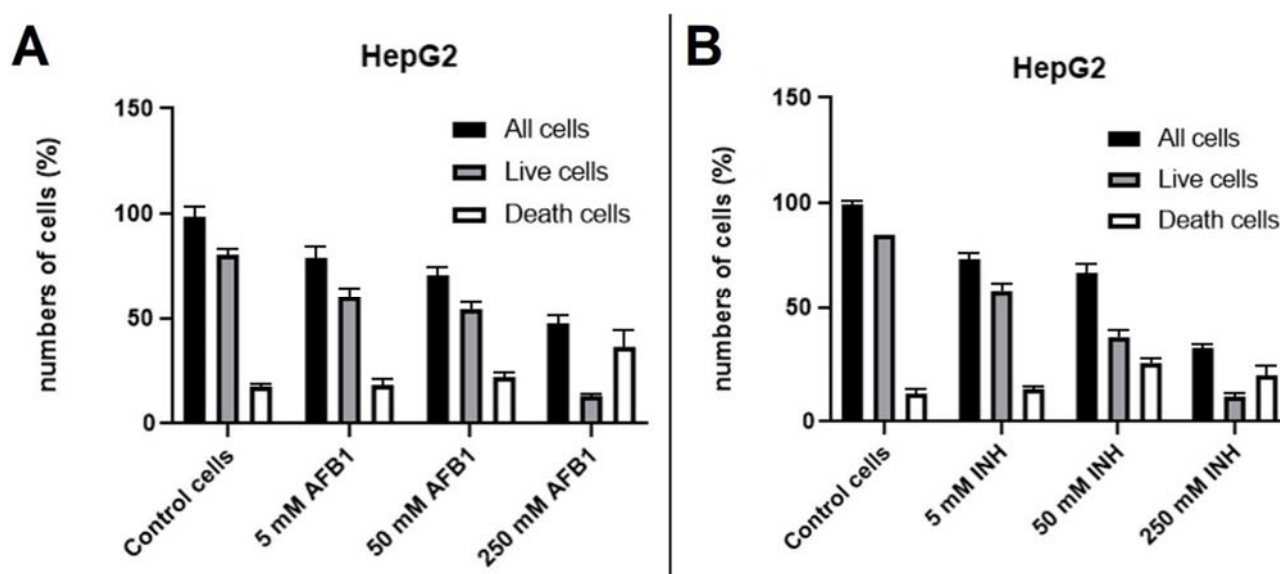


Figure 3. Impact of AFB1 and INH on HepG2 cell survival; graphs of the fluorescent microscopy of HepG2 cells exposed to AFB1 (0, 5, 50, and 250 μ M) (A) and INH (0, 5, 50, and 250 mM) (B) at 24 h using the double staining method with Hoechst 33342 and propidium iodide (PI).

3.4. Fluorescence Microscopy

The effect of AFB1 and INH on the morphology of HepG2 cells was studied by scanning electron microscopy (SEM). HepG2 cells were exposed to different concentrations of AFB1 (5, 50, and 250 μ M) and different concentrations of INH (5, 50 in 150 mM) for 48 h. The results are presented separately for AFB1 and INH. Microphotographs at different magnifications are presented in the Supplementary Materials (Figures S4–S7).

3.4.1. Aflatoxin B1

The results indicate that AFB1 at increasing concentrations induces intracellular biochemical events such as skeletal damage, cell growth inhibition, and cell death. Therefore, the results showed distinct morphological changes and decreased cell viability and adhesion to the stainless steel surface with increasing AFB1 concentration. The contrast in the photographs was due to the contrast reagent used in cell fixation. The elongated lines that can be observed in the background of the cells are an example of cold-rolled steel.

Figure 4 shows the SEM microphotographs of HepG2 cells at various concentrations of AFB1 (0, 5, 50, and 250 μ M) at 1000 \times magnification. During morphology investigation, it was observed that the cell surface was composed of flattened cells that interacted closely. At an AFB1 concentration of 5 μ M, a rough and textured cell surface was observed, where cells were more widely spaced and elevated. At an AFB1 concentration of 50 μ M, the cell surface was more clearly altered, roughened, and textured, with the cells becoming flatter and had a spindle or round shape with growths up to 1 μ m in diameter. At an AFB1 concentration of 250 μ M, an even more structured surface with an altered round cell shape was observed, which could indicate that the cell has gone well into smaller structures, described as blebs. These can be identified as the spherical structures observed on the surface of the electrode.

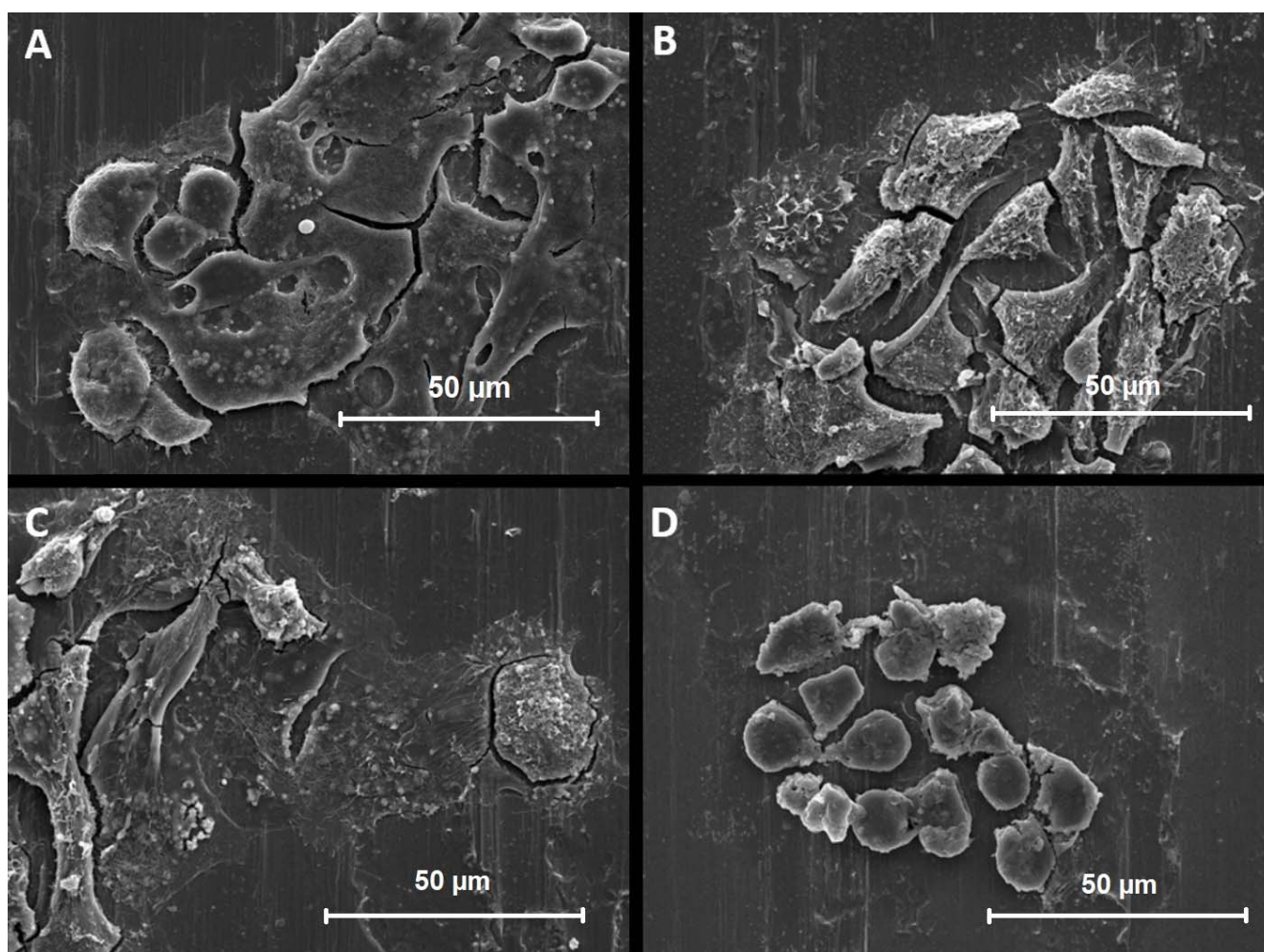


Figure 4. SEM photographs of the HepG2 cells exposed to increasing concentrations of AFB1 at 1000× magnification. HepG2 cells were exposed to different concentrations starting with the control (A), 5 μ M (B), 50 μ M (C), and 250 μ M (D).

3.4.2. Isoniazid

The results show that INH induces intracellular biochemical events such as skeletal damage, cell growth inhibition, and cell death, which can be due to either apoptosis and necrosis, at increasing concentrations. The SEM microphotographs (Figure 5A–D) demonstrate distinct morphological changes such as reduced adhesion, followed by cell disintegration with increasing INH concentration. Similar to the SEM analysis of samples exposed to AFB1, the elongated lines that were observed in the background of the cells are an example of the cold-rolled steel surface.

Figure 5 shows representative SEM figures of HepG2 cells at various concentrations of INH (0, 5, 50, and 250 mM) at 1000× magnification. Again, in the control group, the cells were flattened and interacted closely with each other. At an INH concentration of 5 mM, the cell surface was smooth, more spaced, and stretched, suggesting that their behavior was altered. At 50 mM INH, the HepG2 cells had a noticeable rounder shape with individual vesicular growths of up to 1 μ m. At even increased concentrations of 250 mM, the cell surface was transformed into several individual round clusters, with even more significant vesicular proliferations. Based on the fluorescence microscopy figures, it can be assumed that these spherical cell residues are blebs that formed during the cell death process, which can also be observed as red spots stained with propidine iodide. Despite the cell death, the cell structures appeared to not fully detach and a residue remained on the steel surface.

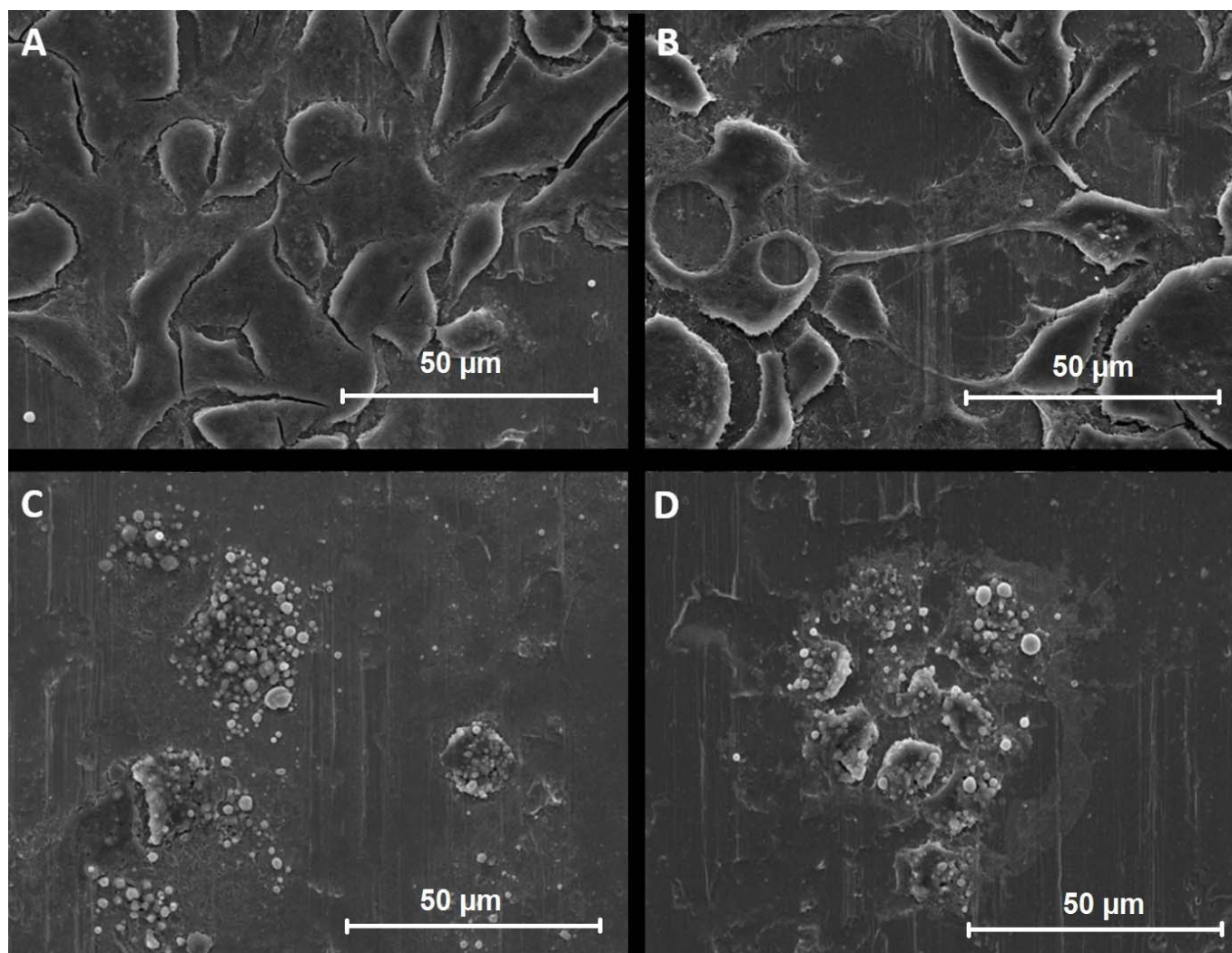


Figure 5. SEM photographs of the HepG2 cells exposed to increasing concentrations of INH at 1000× magnification. HepG2 cells were exposed to different concentrations starting with the control (A), 5 mM (B), 50 mM (C), and 250 mM (D).

3.5. Electrochemical Impedance Spectroscopy

Electrochemical impedance spectroscopy (EIS) measurements were performed to determine the usefulness of adherent HepG2 cells on a stainless steel surface as a biosensing electrochemical device. Both of the Nyquist plots are presented in Figure 6. In all of the EIS figures, the black label represents the negative control where the cells were not affected by hepatotoxin, blue label represents the biosensor with added hepatotoxin, while the red label represents the positive control, where no cells were on the surface. The results show that the negative control, where the cells were on the surface but not exposed to the toxin, had a relatively low total impedance from 120 to 160 $k\Omega\text{ cm}^{-2}$ at low frequencies (below 10 Hz). This difference in impedance can be attributed to cell coverage, where the electrode could have exposed surfaces, resulting in lower impedance. It can be concluded that the coating of the cells on the surface was relatively thin or that the cells did not completely cover the electrode [48]. Despite this, an impedance response could still be observed, since there was a change in exposed metal surface, which affects the general resistance and conductivity of the active surface area. The Nyquist plot showed that the capacitance ($-Z'$) of the negative control was higher than the capacitance of both the investigated samples and the positive control, suggesting that the surface conductivity increased with the addition of hepatotoxin. For AFB1, a test concentration of 250 μM was used, while for INH, a test concentration of 250 mM was used.

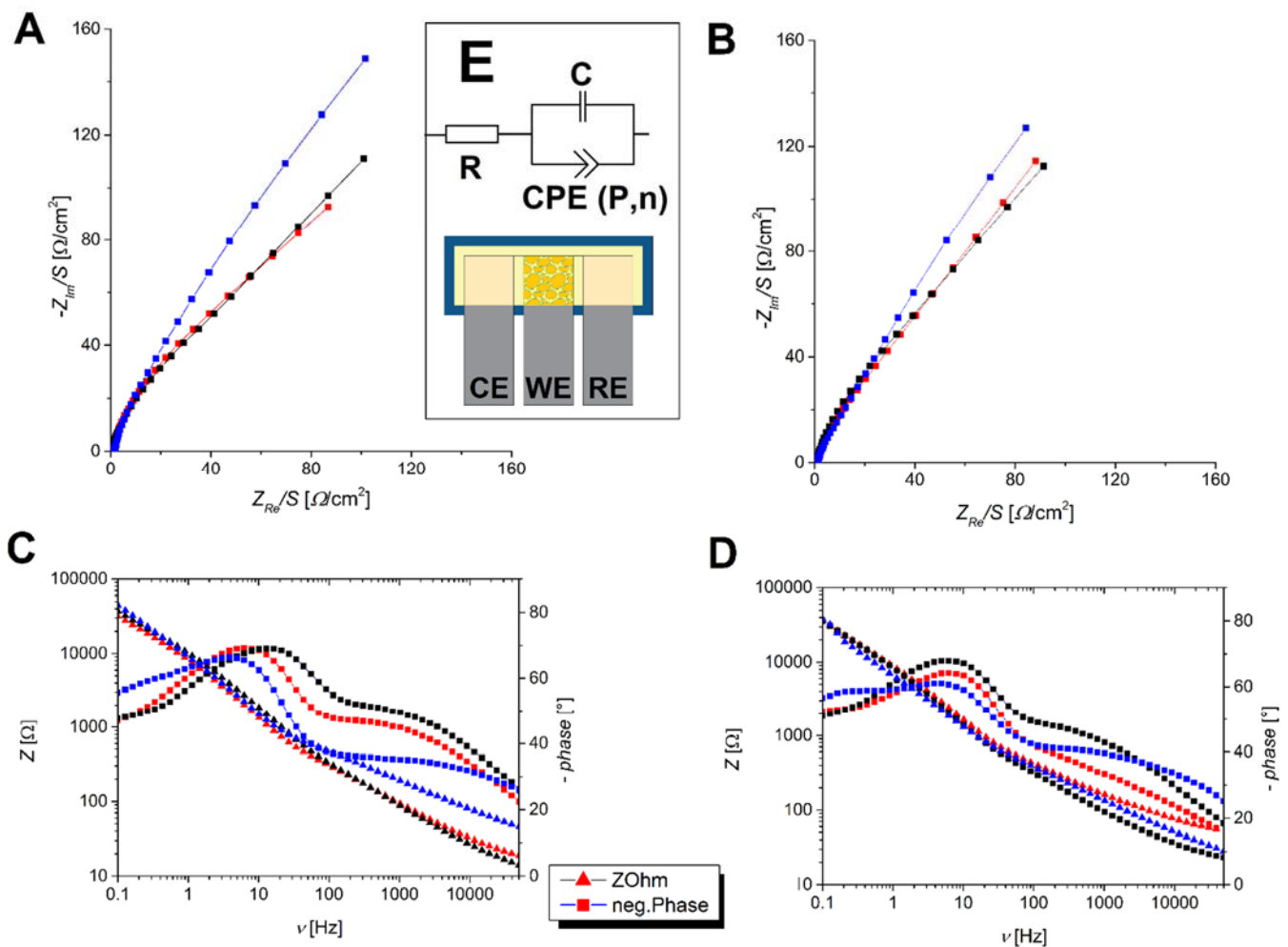


Figure 6. Nyquist diagrams of investigated biosensors showing a response for aflatoxin B1 (A) and isoniazid (B), along with Bode diagrams for aflatoxin B1 (C) and isoniazid (D). For Bode diagrams, triangles represent total impedance $|Z|$, while squares represent phase change. Both biosensors that had applied hepatotoxin are marked with a black label, where the control measurement is marked with the blue label and the biosensor without any attached cells is marked with the red label. Units are Ω/cm^2 where the impedance response is normalized for the surface of the WE. A schematic of the biosensor with electrode placement (E bottom) along with fitted circuit for EIS analysis (E top) is also shown.

In the case of AFB1 testing (Figure 6A), it can be observed that the tested concentration almost aligned with the positive control, suggesting that the surface had been almost completely stripped from the cells. This slightly higher impedance could be attributed to the cell residue and blebs [49] that remain on the surface and can be observed during fluorescence microscopy and SEM studies. From the Bode plot (Figure 6C), it can be observed that overall impedance $|Z|$ had a relatively small change for the duration of measurement, while comparing phase change in frequency range below 1 Hz showed significant differences between the untreated negative control and the treated biosensor. In the case of the treated sample, the response was very similar to the positive control, which had no cells attached onto WE.

In the case of INH testing (Figure 6B), the difference between the negative and positive control was smaller, with a difference between 10 and 20 $\text{k}\Omega\text{ cm}^{-2}$, which is likely due to the lower coverage of HepG1 cells on the steel surface. Furthermore, when measuring the response for INH, this actually had a slightly lower impedance compared to the positive control. The most likely reason for this is the increased conductivity, which could be due

to secondary metabolites, or products that are formed during the necrosis process of the cells [50]. Similar to AFB1 testing, the Bode plot (Figure 6D) showed that overall impedance $|Z|$ remained relatively unchanged between all of the measurements, indicating only a slight change when comparing the negative control, positive control, and sample. Difference in phase angle, however, could be observed, and was visible at frequencies below 1 Hz, indicating a change in the electrode surface.

Finally, the obtained results were modeled using an R [CQ] fitting circuit (Figure 6E), which shows that the electrochemical behavior can be interpreted to the following electrical elements. Despite certain differences, it is expected that the initial resistor R covers the combined effects of the electrolyte and steel surface covered with cells, while the constant phase element (CPE) Q can be attributed toward cell coverage, where capacitor C determines the use of cellulose paper, which acts as a electrolyte holder material. Previous studies have used RQ [51,52] and R [RQ] [53] circuits for fitting, which was also investigated, however, it was observed during the fitting process that the data were better fitted if the parallel resistor was replaced with a capacitor. The tables of fitting results are shown in Tables S1 and S2.

Schematics of the biosensor are shown in Figure 6E, indicating the electrode placement.

The results are consistent with other microscopic observations confirming that both AFB1 and INH damages the HepG2 cells at high concentrations. The data are in agreement with the fitting circuit and previous literature [54], suggesting that the change in impedance is indeed due to changes on the electrode surface [55]. The fitting circuit and spectra are presented in the Supplementary Materials (Figures S8 and S9). It is speculated that due to the relatively uneven coverage and cell gaps on the electrodes, the limit of detection (LOD) is predicted to be quite high for AFB1 and 250 mM for INH, since it was difficult to obtain a signal with a sufficient difference at lower concentrations. In addition, the data showed that it is possible to detect hepatotoxins even with electrodes that are not fully covered with cells, since the response detection is dictated by surface resistance and conductivity change. Therefore, the collected data indicate that it is possible to detect the presence of different types of hepatotoxins, although at relatively high concentrations.

4. Discussion

The cytotoxicity effects of AFB1 and INH on HepG2 cells were investigated along with the ability of HepG2 cells to adhere to the stainless steel surface and the use of the cell covered stainless steel surface in order to be used as an electrochemical biosensor. The HepG2 cells reacted to hepatotoxin aflatoxin B1 (AFB1) and isoniazid (INH) regardless of the adhered surface (glass or steel). In cytotoxic assays, AFB1, at a concentration above 10 μM , and INH at a concentration above 10 mM, were found to significantly reduce the viability of HepG2 cells. These results were further confirmed using fluorescence microscopy. The number of all cells in the total cell population and the number of live HepG2 cells on the steel surface after exposure to increasing concentrations of AFB1 (0, 5, 50, and 250 μM) and INH (5, 50, and 150 mM) decreased, while the number of dead cells gradually increased with increasing concentrations of AFB1 (0, 5, 50, and 250 μM) and INH (0, 5, 50, and 150 mM). With a fluorescence microscope, it was observed that the cell population control had relatively good coverage of the steel surface, while HepG2 cells gradually decreased after exposure to increasing concentrations of the toxins AFB1 and INH. With optical microscopy, it was also observed that the cells used in the negative control sample achieved good statistical coverage of the plate surface. This indicates that the concept of adhering cells to the metal surface is plausible and enables its initial use as an electrode material while HepG2 cells showed decreasing coverage of the plate after being exposed to increasing INH and AFB1 concentrations. Using scanning electron microscopy (SEM), it was observed that the toxin affects the morphology, adhesion, and coverage with adhered HepG2 cells of metal electrodes. At increasing concentrations, AFB1 and INH cause intracellular biochemical events such as skeletal damage, cell growth inhibition, and cell death. Therefore, the SEM figures showed distinct morphological changes and a decrease in cell viability and adhesion to the steel surface with increasing concentrations of

the toxins. The electrochemical impedance spectroscopy results are consistent with other microscopic observations, confirming that INH at high concentrations damages HepG2 cells, and consequently, they no longer cover the metal surface. From the data collected, it can be concluded that a biosensor using live HepG2 cells could successfully detect the presence of INH at a relatively high concentration of 150 mM as well as for AFB1 at concentrations exceeding 250 μ M. Overall, the device demonstrated the ability to determine if it was exposed to hepatotoxins.

5. Conclusions

All of the obtained results support the hypothesis that HepG2 cells can adhere to the metal surface. It was shown that the prepared metal electrodes with adhered cells could be used as part of the biosensor to determine simple hepatotoxic samples. Despite the fact that these concentrations were substantially higher than the ones that showed effects on cell viability in the cytotoxicity test, the cell-covered electrode successfully showed that it could detect both AFB1 and INH. In addition, such biosensors could be, with minimal modifications, used to detect other hepatotoxins such as mycotoxins and could be used as an effective tool in food industries or forensics. In addition, the results suggest that in the future, it may be possible to use metal electrodes with attached living cells for practical biosensors that could be generally useful in medical diagnostics or environmental monitoring. An impedance biosensor could be used for different cell types (lung, nasal, skin, nerve cells, and others) that could probe different types of toxins and pathogens specific to the type of target disease or suspected toxin in the environment.

Supplementary Materials: The following are available online at <https://www.mdpi.com/article/10.3390/bios12030160/s1>, Figure S1: Resazurin assay; Figures S2 and S3: Fluorescence microscopy; Figures S4–S7: SEM microscopy; Figures S8 and S9: EIS fitting; Tables S1 and S2: Fitting data.

Author Contributions: Conceptualization, D.D. and M.R.; Methodology, M.R., D.D. and A.S.; Software, Z.Š.; Validation, A.S., M.R., A.P. and U.B.; Formal analysis, A.S. and M.R.; Investigation, A.S., M.H. and M.R.; Resources, D.D. and A.P.; Data curation, M.R. and Z.Š.; Writing—original draft preparation, M.R. and Z.Š.; Writing—review and editing, M.R. and Z.Š.; Visualization, M.R.; Supervision, A.P., D.D. and U.B.; Project administration, D.D. and U.B.; Funding acquisition, U.B. All authors have read and agreed to the published version of the manuscript.

Funding: This research was funded by the Slovenian Research Agency (ARRS): core project number J1-2471, J1-9162, P1-0207, and P2-0046. This paper is part of the dissemination activities of the project FunGlass. This project received funding from the European Union's Horizon 2020 research and innovation program under grant agreement no. 739566.

Institutional Review Board Statement: Not applicable.

Informed Consent Statement: Not applicable.

Data Availability Statement: Data are available directly from the authors upon reasonable request.

Acknowledgments: Ajda Sušnik would like to thank Venko Kononenko for help with the microscopy measurements. Martin Rozman would like to thank Felix Rozman for the general discussion.

Conflicts of Interest: The authors declare no conflict of interest.

References

1. Duan, L.; Akakpo, J.Y.; Ramachandran, A.; Jaeschke, H. Environmental liver toxins. In *Encyclopedia of Environmental*, 2nd ed.; Elsevier: Oxford, UK, 2019; pp. 578–584.
2. Zhu, L.; Huang, C.; Yang, X.; Zhang, B.; He, X.; Xu, W.; Huang, K. Proteomics reveals the alleviation of zinc towards aflatoxin b1-induced cytotoxicity in human hepatocytes (hepg2 cells). *Ecotoxicol. Environ. Saf.* **2020**, *198*, 110596. [[CrossRef](#)] [[PubMed](#)]
3. Štern, A.; Furlan, V.; Novak, M.; Štampar, M.; Kolenc, Z.; Kores, K.; Filipič, M.; Bren, U.; Žegura, B. Chemoprotective effects of xanthohumol against the carcinogenic mycotoxin aflatoxin b1. *Foods* **2021**, *10*, 1331. [[CrossRef](#)] [[PubMed](#)]
4. Tabata, S. Mycotoxins: Aflatoxins and related compounds. In *Encyclopedia of Dairy Sciences*, 3rd ed.; Elsevier: Amsterdam, The Netherlands, 2022; pp. 575–585.

5. Flament, E.; Guitton, J.; Gaulier, J.; Gaillard, Y. Human poisoning from poisonous higher fungi: Focus on analytical toxicology and case reports in forensic toxicology. *Pharmaceuticals* **2020**, *13*, 454. [[CrossRef](#)] [[PubMed](#)]
6. Wilson, C.R.; Butz, J.K.; Mengel, M.C. Methods for analysis of gastrointestinal toxicants. In *Reference Module in Biomedical Sciences*; Elsevier: Amsterdam, The Netherlands, 2014.
7. Wong, A.; Graudins, A. Risk prediction of hepatotoxicity in paracetamol poisoning. *Clin. Toxicol.* **2017**, *55*, 879–892. [[CrossRef](#)]
8. YEW, W.W.; LEUNG, C.C. Antituberculosis drugs and hepatotoxicity. *Respirology* **2006**, *11*, 699–707. [[CrossRef](#)]
9. Hassan, H.M.; Guo, H.-I.; Yousef, B.A.; Luyong, Z.; Zhenzhou, J. Hepatotoxicity mechanisms of isoniazid: A mini-review. *J. Appl. Toxicol.* **2015**, *35*, 1427–1432. [[CrossRef](#)]
10. Combrink, M.; Loots, D.T.; du Preez, I. Metabolomics describes previously unknown toxicity mechanisms of isoniazid and rifampicin. *Toxicol. Lett.* **2020**, *322*, 104–110. [[CrossRef](#)]
11. McElhiney, J.; Lawton, L.A. Detection of the cyanobacterial hepatotoxins microcystins. *Toxicol. Appl. Pharmacol.* **2005**, *203*, 219–230. [[CrossRef](#)]
12. Ye, W.; Liu, T.; Zhang, W.; Zhu, M.; Liu, Z.; Kong, Y.; Liu, S. Marine toxins detection by biosensors based on aptamers. *Toxins* **2019**, *12*, 1. [[CrossRef](#)]
13. Tothill, I.E.; Turner, A.P.F. Biosensors. In *Encyclopedia of Food Sciences and Nutrition*, 2nd ed.; Academic Press: Oxford, UK, 2003; pp. 489–499.
14. Caballero, B.; Trugo, L.C.; Finglas, P.M. *Encyclopedia of Food Sciences and Nutrition*; Elsevier: Amsterdam, The Netherlands, 2003.
15. Bhalla, N.; Jolly, P.; Formisano, N.; Estrela, P. Introduction to biosensors. *Essays Biochem.* **2016**, *60*, 1–8. [[CrossRef](#)]
16. Malhotra, S.; Verma, A.; Tyagi, N.K.; Kumar, V. Biosensors: Principle, types and applications. *Int. J. Adv. Res. Innov. Ideas Educ.* **2017**, *3*, 3639–3644.
17. Karim, F.; Fakhruddin, A.N.M. Recent advances in the development of biosensor for phenol: A review. *Rev. Environ. Sci. Biotechnol.* **2012**, *11*, 261–274. [[CrossRef](#)]
18. Amaro, F.; Turkewitz, A.P.; Martı́n-González, A.; Gutiérrez, J.C. Functional GFP-metallothionein fusion protein from tetrahymena thermophila: A potential whole-cell biosensor for monitoring heavy metal pollution and a cell model to study metallothionein overproduction effects. *BioMetals* **2014**, *27*, 195–205. [[CrossRef](#)] [[PubMed](#)]
19. Courbet, A.; Endy, D.; Renard, E.; Molina, F.; Bonnet, J. Detection of pathological biomarkers in human clinical samples via amplifying genetic switches and logic gates. *Sci. Transl. Med.* **2015**, *7*, 283–289. [[CrossRef](#)]
20. Goers, L.; Ainsworth, C.; Goey, C.H.; Kontoravdi, C.; Freemont, P.S.; Polizzi, K.M. Whole-cell escherichia coli lactate biosensor for monitoring mammalian cell cultures during biopharmaceutical production. *Biotechnol. Bioeng.* **2017**, *114*, 1290–1300. [[CrossRef](#)]
21. Wang, N.; Wang, H.; Zhang, J.; Ji, X.; Su, H.; Liu, J.; Wang, J.; Zhao, W. Diketopyrrolopyrrole-based sensor for over-expressed peroxynitrite in drug-induced hepatotoxicity via ratiometric fluorescence imaging. *Sens. Actuators B Chem.* **2022**, *352*, 130992. [[CrossRef](#)]
22. Lu, W.; Huang, B.; He, Y.; Yang, J.; Li, Y. A facile cell-involved microfluidic platform for assessing risk of hepatotoxic chemicals via on-line monitoring of multi-indexes. *Sens. Actuators B Chem.* **2021**, *341*, 129938. [[CrossRef](#)]
23. Zhang, X.; Hatamie, A.; Ewing, A.G. Nanoelectrochemical analysis inside a single living cell. *Curr. Opin. Electrochem.* **2020**, *22*, 94–101. [[CrossRef](#)]
24. Zhou, W.; Graham, K.; Lucendo-Villarin, B.; Flint, O.; Hay, D.C.; Bagnaninchi, P. Combining stem cell-derived hepatocytes with impedance sensing to better predict human drug toxicity. *Expert Opin. Investig. Drugs* **2019**, *15*, 77–83. [[CrossRef](#)]
25. Gupta, N.; Renugopalakrishnan, V.; Liepmann, D.; Paulmurugan, R.; Malhotra, B.D. Cell-based biosensors: Recent trends, challenges and future perspectives. *Biosens. Bioelectron.* **2019**, *141*, 111435. [[CrossRef](#)]
26. Javitt, N.B. Hep g2 cells as a resource for metabolic studies: Lipoprotein, cholesterol, and bile acids. *FASEB J.* **1990**, *4*, 161–168. [[CrossRef](#)] [[PubMed](#)]
27. Westerink, W.M.A.; Schoonen, W.G.E.J. Cytochrome p450 enzyme levels in hepg2 cells and cryopreserved primary human hepatocytes and their induction in hepg2 cells. *Toxicol. In Vitro* **2007**, *21*, 1581–1591. [[CrossRef](#)] [[PubMed](#)]
28. Guo, L.; Dial, S.; Shi, L.; Branham, W.; Liu, J.; Fang, J.-L.; Green, B.; Deng, H.; Kaput, J.; Ning, B. Similarities and differences in the expression of drug-metabolizing enzymes between human hepatic cell lines and primary human hepatocytes. *Drug Metab. Dispos.* **2011**, *39*, 528–538. [[CrossRef](#)] [[PubMed](#)]
29. Zanchetta, G.; Lanfranco, R.; Giavazzi, F.; Bellini, T.; Buscaglia, M. Emerging applications of label-free optical biosensors. *J. Nanophotonics* **2017**, *6*, 627–645. [[CrossRef](#)]
30. Chen, N.H.; Tomita, U.; Kasagi, N.; Nagamune, T.; Suzuki, Y. Label-free adhesion-based cell sorter using optimized oblique grooves for early cancer detection. In Proceedings of the 2011 IEEE 24th International Conference on Micro Electro Mechanical Systems, Cancun, Mexico, 23–27 January 2011; pp. 904–907.
31. Fang, Y. Label-free biosensors for cell biology. *Int. J. Electrochem.* **2011**, *2011*, 460850. [[CrossRef](#)]
32. Yáñez-Sedeño, P.; Agúí, L.; Campuzano, S.; Pingarrón, J.M. What electrochemical biosensors can do for forensic science? Unique features and applications. *Biosensors* **2019**, *9*, 127. [[CrossRef](#)]
33. Zhang, J.; Lu, L.; Zhang, Z.; Zang, L. Electrochemical cell-based sensor for detection of food hazards. *Micromachines* **2021**, *12*, 837. [[CrossRef](#)]

34. Reshetilov, A.; Arlyapov, V.; Alferov, V.; Reshetilova, T. Bod biosensors: Application of novel technologies and prospects for the development. In *State of the Art in Biosensors—Environmental and Medical Applications*; Rincken, T., Ed.; Intech: Rijeka, Croatia, 2013; pp. 57–77.
35. Săndulescu, R.; Tertiș, M.; Cristea, C.; Bodoki, E. New materials for the construction of electrochemical biosensors. In *Biosensors—Micro and Nanoscale Applications*; Rincken, T., Ed.; Intech: Rijeka, Croatia, 2015; pp. 1–36.
36. Brett, C. Electrochemical impedance spectroscopy for characterization of electrochemical sensors and biosensors. *ECS Trans.* **2019**, *13*, 67–80. [[CrossRef](#)]
37. Jaffrezic-Renault, N. Impedimetric measurements and the biomatrix. In *Encyclopedia of Interfacial Chemistry*; Wandelt, K., Ed.; Elsevier: Oxford, UK, 2018; pp. 241–247.
38. Trentin, A.; Harb, S.V.; Uvida, M.C.; Marcoen, K.; Pulcinelli, S.H.; Santilli, C.V.; Terry, H.; Hauffman, T.; Hammer, P. Effect of ce(III) and ce(IV) ions on the structure and active protection of pmma-silica coatings on aa7075 alloy. *Corros. Sci.* **2021**, *189*, 109581. [[CrossRef](#)]
39. Meddings, N.; Heinrich, M.; Overney, F.; Lee, J.-S.; Ruiz, V.; Napolitano, E.; Seitz, S.; Hinds, G.; Raccichini, R.; Gaberscek, M.; et al. Application of electrochemical impedance spectroscopy to commercial li-ion cells: A review. *J. Power Sources* **2020**, *480*, 228742. [[CrossRef](#)]
40. Kivirand, K.; Min, M.; Rincken, T. Challenges and applications of impedance-based biosensors in water analysis. In *Biosensors for Environmental Monitoring*; Rincken, T., Kivirand, K., Eds.; Intech: Rijeka, Croatia, 2019; pp. 2–4.
41. Xia, S.; Zhu, P.; Pi, F.; Zhang, Y.; Li, Y.; Wang, J.; Sun, X. Development of a simple and convenient cell-based electrochemical biosensor for evaluating the individual and combined toxicity of don, zen, and afb1. *Biosens. Bioelectron.* **2017**, *97*, 345–351. [[CrossRef](#)] [[PubMed](#)]
42. Repetto, G.; del Peso, A.; Zurita, J.L. Neutral red uptake assay for the estimation of cell viability/cytotoxicity. *Nat. Protoc.* **2008**, *3*, 1125–1131. [[CrossRef](#)]
43. Rodger, A.; Sanders, K. Uv-visible absorption spectroscopy, biomacromolecular applications. In *Encyclopedia of Spectroscopy and Spectrometry*, 3rd ed.; Lindon, J.C., Tranter, G.E., Koppenaal, D.W., Eds.; Academic Press: Oxford, UK, 2017; pp. 495–502.
44. O'Brien, J.; Wilson, I.; Orton, T.; Pognan, F. Investigation of the alamar blue (resazurin) fluorescent dye for the assessment of mammalian cell cytotoxicity. *Eur. J. Biochem.* **2000**, *267*, 5421–5426. [[CrossRef](#)] [[PubMed](#)]
45. Rost, F. Fluorescence microscopy, applications. In *Encyclopedia of Spectroscopy and Spectrometry*; Elsevier: Amsterdam, The Netherlands, 2017; pp. 627–631.
46. Stolwijk, J.A.; Wegener, J. Impedance-based assays along the life span of adherent mammalian cells in vitro: From initial adhesion to cell death. In *Label-Free Monitoring of Cells In Vitro*; Wegener, J., Ed.; Springer International Publishing: Cham, Switzerland, 2019; pp. 1–75.
47. Steinbrecht, S.; Pfeifer, N.; Herzog, N.; Katzenberger, N.; Schulz, C.; Kammerer, S.; Küpper, J.-H. Hepg2-1a2 c2 and c7: Lentivirus vector-mediated stable and functional overexpression of cytochrome p450 1a2 in human hepatoblastoma cells. *Toxicol. Lett.* **2020**, *319*, 155–159. [[CrossRef](#)] [[PubMed](#)]
48. Lukic, S.; Wegener, J. Impedimetric monitoring of cell-based assays. *eLS* **2015**. [[CrossRef](#)]
49. Asphahani, F.; Thein, M.; Wang, K.; Wood, D.; Wong, S.S.; Xu, J.; Zhang, M. Real-time characterization of cytotoxicity using single-cell impedance monitoring. *Analyst* **2012**, *137*, 3011–3019. [[CrossRef](#)] [[PubMed](#)]
50. Lee, R.M.; Choi, H.; Shin, J.-S.; Kim, K.; Yoo, K.-H. Distinguishing between apoptosis and necrosis using a capacitance sensor. *Biosens. Bioelectron.* **2009**, *24*, 2586–2591. [[CrossRef](#)] [[PubMed](#)]
51. Nguyen, B.T.T.; Peh, A.E.K.; Chee, C.Y.L.; Fink, K.; Chow, V.T.K.; Ng, M.M.L.; Toh, C.-S. Electrochemical impedance spectroscopy characterization of nanoporous alumina dengue virus biosensor. *Bioelectrochemistry* **2012**, *88*, 15–21. [[CrossRef](#)]
52. Chen, X.; Wang, Y.; Zhou, J.; Yan, W.; Li, X.; Zhu, J.-J. Electrochemical impedance immunosensor based on three-dimensionally ordered macroporous gold film. *Anal. Chem.* **2008**, *80*, 2133–2140. [[CrossRef](#)]
53. Maalouf, R.; Fournier-Wirth, C.; Coste, J.; Chebib, H.; Saikali, Y.; Vittori, O.; Errachid, A.; Cloarec, J.-P.; Martelet, C.; Jaffrezic-Renault, N. Label-free detection of bacteria by electrochemical impedance spectroscopy: Comparison to surface plasmon resonance. *Anal. Chem.* **2007**, *79*, 4879–4886. [[CrossRef](#)]
54. Bouafsoun, A.; Othmane, A.; Jaffrezic-Renault, N.; Kerkeni, A.; Thoumire, O.; Prigent, A.F.; Ponsonnet, L. Impedance endothelial cell biosensor for lipopolysaccharide detection. *Mater. Sci. Eng. C* **2008**, *28*, 653–661. [[CrossRef](#)]
55. Daza, P.; Olmo, A.; Cañete, D.; Yúfera, A. Monitoring living cell assays with bio-impedance sensors. *Sens. Actuators B Chem.* **2013**, *176*, 605–610. [[CrossRef](#)]